Separation of plasmon-polariton modes of small metal particles

U. Kreibig
Fachbereich 11—Physik, Universität des Saarlandes, D-6600 Saarbrücken, West Germany

B. Schmitz and H. D. Breuer
Fachbereich 13—Physikalische Chemie, Universität des Saarlandes, D-6600 Saarbrücken, West Germany
(Received 8 June 1987)

The plasmon-polariton bands excited optically in Ag-particle systems of various particle sizes were separated by applying both optical and photothermal spectroscopy. The dipolar absorption band, the dipolar scattering band, and the quadrupolar absorption band could be clearly resolved. The essential spectral features confirm the predictions of Mie's electromagnetic theory. Results are also shown for densely packed particle systems.

The excitation of plasmon polaritons in small metal particles gives rise to complex optical extinction spectra consisting both of true absorption and of scattering. In the present contribution we show the experimental separation of such scattering and absorption losses. The optical extinction of spherical particles was calculated already at the beginning of this century by Mie and Debye within the frame of Maxwell's theory, and only a few extensions due to longitudinal excitation modes[1] and due to the size-dependent dielectric response of the particle material[2] have been added since then (some reviews are given in Ref. 3).

Mie and Debye used Rayleigh's partial-wave method assuming various excitation modes in the particles. (For simplicity we use the term "mode" though, in fact, there are polariton states.) These modes due to different multipolar excitations were classified by the multipole order ν of the spherical functions. They are divided into "electric" and "magnetic" modes with the radial components of the magnetic and electric fields $\mathbf{B}_R$ and $\mathbf{E}_R$, respectively, vanishing at the particle surface. The former are interpreted as surface plasmon polaritons, the latter are interpreted as due to eddy currents.

As shown in Table I, the excitation losses of each mode consist both of true absorption A_ν within the particles (by transformation of radiation energy into heat) and of scattering S_ν from the plane incident wave into the full solid angle (conserving the total radiation energy). The total extinction spectrum is thus given by $E(\omega)=\sum_\nu(A_\nu + A'_\nu + S_\nu + S'_\nu)$. The losses due to electric modes form distinct spectral bands if the particle material contains nearly free electrons as, e.g., do the noble metals. The heights, widths, and spectral positions of the A and S bands strongly depend on the particle radius R and on the optical material functions. They are extraordinarily narrow in the special case of Ag particles. The very complex particle-size dependence of the peak heights is shown in Fig. 1, the numerical values corresponding to Ag particles.[4] Below sizes of about 10 nm additional size dependences enter, caused by finite-size effects in the optical material functions.[2] To escape these complications we only deal with larger particles. For $2R \lesssim 20$ nm (i.e., $R/\lambda \lesssim 0.03$, λ the peak wavelength) only the dipolar absorption A_1 is important, which sometimes is called the Fröhlich mode. When R grows, retardation effects become increasingly important and so do the radiative losses S_ν. At $2R \sim 30$ nm S_1 exceeds A_1. Further increase of R lets the higher-multipole contributions $A_2, S_2, A_3, S_3, \ldots$ increase in succession and afterwards decrease again. The angular dependence of the scattering intensity, as predicted by Mie, has been confirmed by detailed measurements of Fragstein *et al.*[5] Since the magnetic contributions S'_ν and A'_ν do not exhibit narrow resonance bands and their contribution is small in the investigated particle-size and spectral region, they are not considered further. Figure 1 merely demonstrates the behavior of the band heights; at the same time, the bandwidths increase and the bands are shifted towards lower frequencies when the particles grow. Both the height and width of the S_1 band remain predominant for all larger sizes in Fig. 1 and, hence, extinction spectra of the larger particles are always governed by S_1. This band superimposes the higher-multipole contributions, which thus cannot be clearly observed and separated in measured extinction spectra. A separation is possible, however, as shown below, by combining different spectroscopic methods.

In the following we present experimental results of a separation of these different loss bands. We chose systems of Ag particles with different mean particle diameters of 19 and 63 nm which were embedded in a solid gelatin matrix.[6] The used samples are portrayed in the electron micrographs of Figs. 2 and 3. The particles have moderate size-distribution width and isometric shapes. The size distributions, also given in Figs. 2 and 3, were determined from the same samples which had before been used for the optical investigations. Medium particle packing densities of about 0.1 were necessary for the optical experiments. Yet, because of separating gelatin coatings around the single particles,[6] densely packed clusters of touching particles were rare, if present at all. (Figures 2 and 3 show particles of several overlying layers which, in the projection, appear not to be separated from each other.)

TABLE I. Decomposition of the extinction of spherical metal particles into true absorption and scattering losses of various multipolar modes (ν: mode index; $\mathbf{E}_R, \mathbf{B}_R$: electric and magnetic radial field at the particle surface).

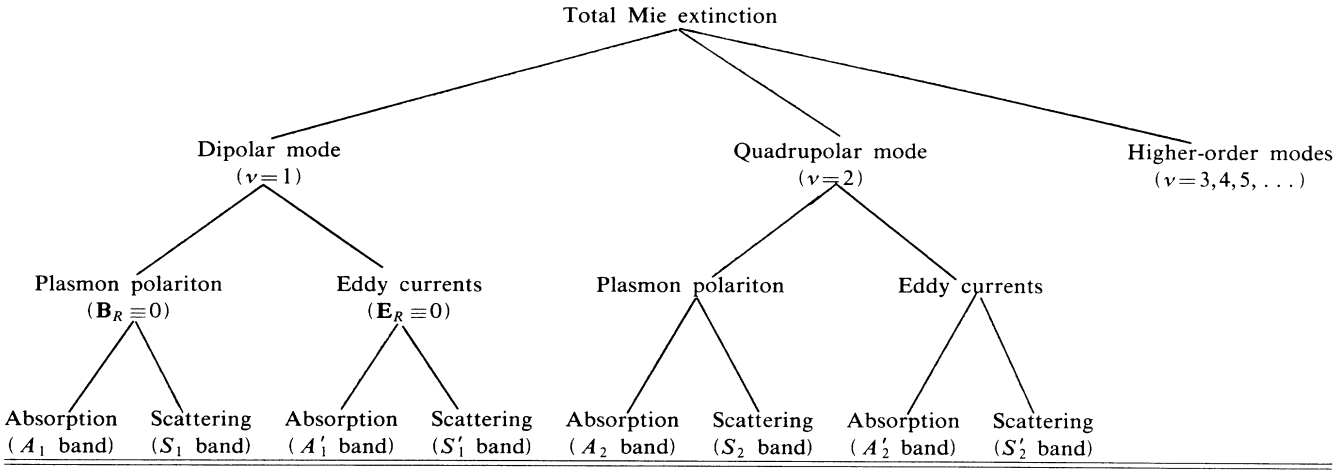

Two optical loss spectroscopy methods were applied to the samples: First, total extinction spectra were recorded with a conventional transmission spectrophotometer from the two samples with different mean particle sizes [Figs. 2(b) and 3(b), thin lines]. Second, pure absorption spectra were measured by photothermal deflection spectroscopy.[7] In these experiments the samples are irradiated with the intensity-modulated radiation of a high-intensity xenon light source with monochromator. True optical absorption due to radiationless deactivation processes in the sample produces a slight increase of the sample temperature and also of the air-gas layer adjacent to the sample surface. As a consequence, the refractive index of the gas layer decreases and a laser beam traveling at a small distance parallel to the sample surface is slightly deflected when passing through the hot-gas "lens." The magnitude of this deflection, measured with a position-sensitive Si detector, is related to the absorption constant of the material under investigation. To good approximation, both prove to be proportional in the intensity range of the present experiments.[7] The two true absorption spectra shown in Figs. 2(b) and 3(b) with thick lines were thus recorded by tuning the frequency of the incident light.

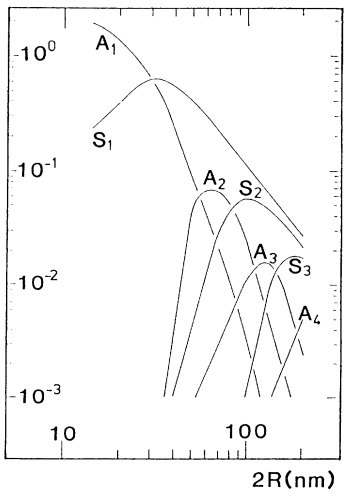

FIG. 1. Maxima of the absorption (A_ν) and scattering (S_ν) bands composing the optical extinction of spherical Ag particles, as functions of the particle diameter $2R$. ν: order of the multipole; computed from Mie's theory (figure taken from Ref. 2); optical material constants of bulk material.

The same samples were used both for the extinction and for the photothermal measurements and were afterwards characterized by electron microscopy. So the spectra of both experiments can be directly compared. While in the case of the smaller particles both kinds of spectra coincide in the main (the width of the photothermal band being somewhat larger due to the broad spectral width of the incident light of about ± 0.1 eV), the two spectra of the larger particles differ markedly from each other. The differences will be explained in the following by comparing the measured spectra with the corresponding computed Mie spectra. The computations were performed by including all modes up to $\nu=5$ and by taking the particle-size distributions of Figs. 2 and 3 into account. The resulting extinction spectra and their decomposition into A_ν and S_ν bands are shown in Figs. 2(a) and 3(a).

Figure 2(a) shows that the *extinction* of the 19-nm particles mainly consists of the absorption A_1 of the dipolar mode centered at 3.0 eV. Additional weak contributions are due to S_1. Thus it is expected that the corresponding *photothermal* spectrum consisting of the A_1 band only, essentially coincides with the extinction. The experimental spectra in Fig. 2(b) clearly confirm this prediction.

On the other hand, Fig. 3(a) shows that, in contrast to this first case, the computed spectra differ strongly for the 63-nm particles. Now, the *extinction* spectrum is mainly due to the dipolar radiative losses S_1, which form a very broad band centered at about 2.6 eV. S_1 exceeds the dipolar absorption A_1 by half an order of magnitude, the latter being shifted downward to 2.7 eV and markedly broadened compared to the small-particle case.

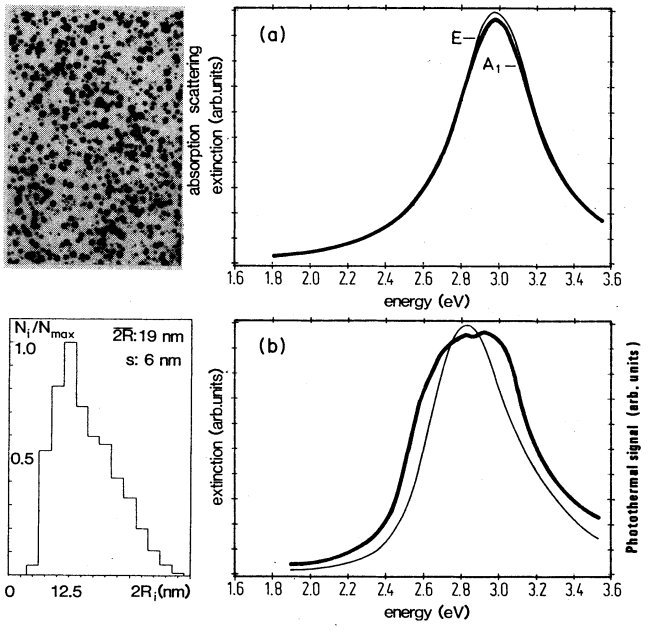

FIG. 2. Computed and measured optical spectra of a sample of small Ag particles ($\overline{2R}=19\pm6$ nm). The left-side figures show a TEM picture and the size distribution of the measured sample. (a) Computed Mie extinction (E) and dipolar absorption (A_1). (Filling factor $=10^{-6}$; size distribution included; dielectric constant of the matrix is 2.37; see Ref. 10). (b) Measured extinction spectrum (thin line) and photothermal spectrum (bold line).

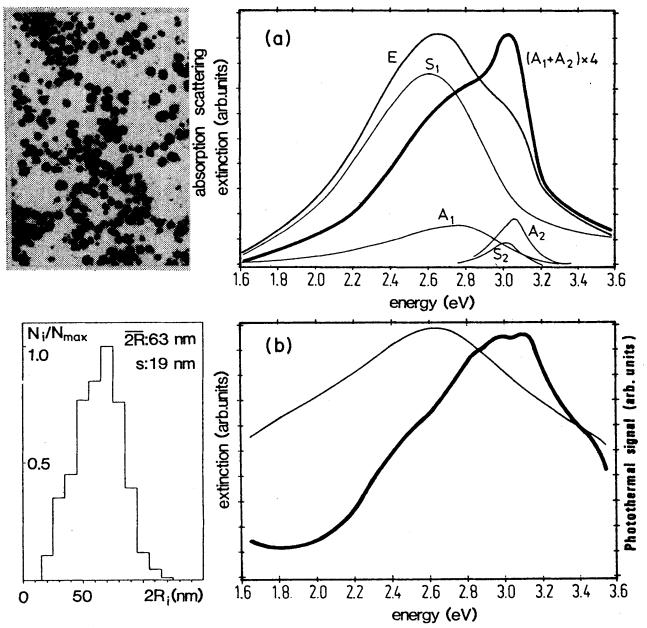

FIG. 3. Computed and measured optical spectra of a sample of larger Ag particles ($\overline{2R}=63\pm19$ nm). The left-side figures show a TEM picture and the size distribution of the measured sample. (a) Computed Mie extinction (E) and the contributions of the ν-polar absorption (A_ν) and scattering (S_ν) bands. The total true absorption is plotted on an $4\times$ enlarged scale (bold line). (Filling factor is 10^{-6}; size distribution included; dielectric constant of the matrix is 2.37). (b) Measured extinction spectrum (thin line) and photothermal spectrum (bold line).

In addition, the quadrupolar absorption A_2 forms a narrow band at 3.1 eV. Both A_1 and A_2 are superimposed by large S_1 contributions. The extinction is slightly increased further by a small S_2 contribution. All other excitations—including the magnetic ones—are too weak to show up in this figure.

The pure absorptive losses A_1+A_2 are plotted once more on an enlarged scale in Fig. 3(a) (bold curve). This spectrum shows what one would suppose for the photothermal measurement, where scattering losses S_1 and S_2 are expected to be absent. The two experimental spectra of Fig. 3(b) follow the expected behavior: there is a very broad *extinction* band centered at about 2.6 eV, which thus is identified as mainly due to the dipolar radiative losses S_1. The width of the measured extinction band surpasses somewhat the computed one, probably because of dense-packing-effects in the particle system. These effects have been discussed earlier in detail (e.g., Refs. 6–9). It should be pointed out that these effects are too small in our samples to make the identification of the bands uncertain. This is proven by the experimental results of the 19-nm particles, Fig. 2(b), which do not show marked packing effects, notwithstanding that the particle-packing density in these samples was somewhat higher than in the 63-nm particle samples. Packing effects would have resulted in increased extinction at the low-frequency flank of the spectrum in Fig. 2(b), i.e., deviations from the symmetric shape of the extinction band. The samples were thin enough to avoid serious multiple-scattering effects.

Comparing the bold curves of Figs. 3(a) and 3(b), it is obvious that the measured *photothermal* spectrum has the very structure predicted by the computed true absorption spectrum A_1+A_2. So its main band, centered at 3.1 eV, is identified as the quadrupolar absorption A_2 and the broad structure at its low-energy flank is due to the broad dipolar absorption A_1 around 2.6 eV. The peak-height ratio is roughly 1:2, i.e., the value expected for the absorption bands A_1 and A_2. Scattering losses are not indicated in the photothermal spectrum (though, of course, scattering takes place in this experiment too).

We were thus able, by applying both extinction and photothermal spectroscopy to the same samples, to separate and identify the quadrupolar plasmon-polariton absorption A_2 which in conventional extinction measurements is covered by the larger dipolar scattering. This latter contribution S_1 could, in principle, be separated, as well, by subtracting both kinds of spectra after appropriate weighting of their strengths.

Finally, we show in Fig. 4 analogous spectra of a thick sample of small Ag particles ($\overline{2R}=10$ nm), the packing density of which is extremely high (filling factor ~0.4). In this sample particle *aggregates* of widely varying structures and sizes are formed. Now, electromagnetic particle-particle interaction effects and multiple scattering effects strongly influence the extinction, causing the extinction spectrum to cover the whole visible range and even to extend far into the ir region. Due to coherence

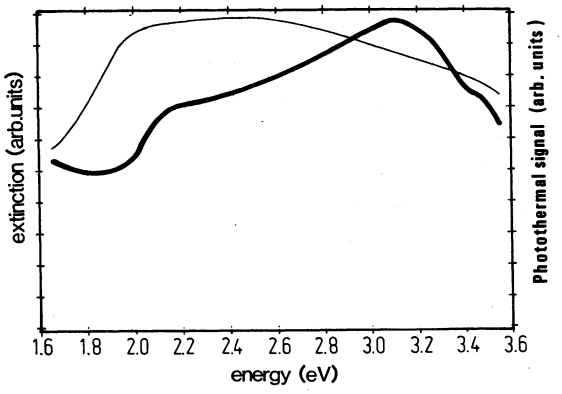

FIG. 4. Measured optical extinction spectrum (thin line) and photothermal spectrum (thick line) of a sample of densely packed Ag particles. Mean particle diameter $\overline{2R} = 10$ nm; filling factor ~ 0.4.

effects, the scattered light of such samples already approaches regular reflectance.

Despite extended investigations of the optical properties of such dense many-particle systems (e.g., Refs. 6, 8, and 9), which are determined by absorption and scattering of various multipolar *aggregate* modes, the extinction spectrum of the latter very complex sample cannot yet be synthesized by calculations. Some information, however, can be drawn by comparing the extinction (thin line) and the absorption spectrum (thick line) of Fig. 4. In the low-frequency region the largest contribution to the extinction obviously stems from scattering losses since the relative extinction contributions markedly exceed the pure absorption. It would be of interest to investigate whether this also holds in the far ir region. It should be pointed out that Ag particles of the same small size, but well separated in dilute systems of low filling factor, would not show any scattering at all. By the way, these scattering losses are disregarded in all model calculations of aggregate spectra based upon the quasistatic-field approximation.

The position of the main peak of true absorption in Fig. 4 is in the high-energy region and nearly coincides with that of the single small particle [Fig. 2(a)]. In this region aggregated Ag particles have their high-frequency aggregate modes.[6] The extended and asymmetric shape of the low-frequency flank of the photothermal spectrum points to a large number of different low-frequency *aggregate* modes. Probably this flank is additionally lifted somewhat by multiple extinction effects.

To summarize, we have shown experimentally the optical extinction spectra of Ag particles to consist of distinct absorption and scattering loss bands, and for the first time it was possible to separate clearly the development of the quadrupolar spherical plasmon polariton as the particle size is increased. It appears promising to extend the present analysis to the ir and far ir regions (e.g., by using samples with roughened surface structures which might be measured more sensitively by photoacoustic than by photothermal spectroscopy methods), to investigate the relative contributions of absorption and scattering to the extinction observed in these spectral regions for densely packed and/or aggregated particle samples.[11]

[1]R. Clanget, Optik **35**, 180 (1972); R. Ruppin, Phys. Rev. B **11**, 2871 (1975).

[2]W. Doyle, Phys. Rev. **111**, 1067 (1958). C. v. Fragstein and H. Roemer, Z. Phys. **151**, 51 (1958); R. Doremus, J. Chem. Phys. **40**, 2389 (1964); **42**, 414 (1965); C. v. Fragstein and F. Schoenes, Z. Phys. **198**, 477 (1967); U. Kreibig and C. v. Fragstein, Z. Phys. **224**, 307 (1969); U. Kreibig, J. Phys. F **4**, 999 (1974).

[3]Reviews of optical properties of small particles; e.g., J. Perenboom, P. Wyder, and F. Maier, Phys. Rep. **78**, 173 (1981); R. Ruppin, *Electromagnetic Surface Modes* (Wiley, New York, 1982), p. 345; C. Bohren and D. Huffman, *Absorption and Scattering of Light by Small Particles* (Wiley, New York, 1983); U. Kreibig, *Contribution of Cluster Physics to Materials Science and Technology*, Vol. E**104**, of NATO Advanced Study Institute, 1982 (Nijhoff, Dordrecht, 1986), p. 373; U. Kreibig and L. Genzel, Surf. Sci. **156**, 678 (1985).

[4]U. Kreibig and P. Zacharias, Z. Phys. **231**, 128 (1970).

[5]C. v. Fragstein, J. Meingast, and H. Hoch, Forschungsber. Wirtsch. Verkehrminist. Nordrhein-Westfalen, **174** (1955).

[6]U. Kreibig, A. Althoff, and H. Pressmann, Surf. Sci. **106**, 308 (1981); D. Schönauer, and U. Kreibig, Surf. Sci. **156**, 100 (1985).

[7]W. Jackson, N. Amer, A. Boccara, and D. Fournier, Appl. Opt. **20**, 1333 (1981).

[8]U. M. Gerardy and M. Ausloos, Phys. Rev. B **22**, 4950 (1980); *ibid.* **25**, 4204 (1982); **27**, 6446 (1983); G. Niklasson and C. G. Granqvist, J. Appl. Phys. **55**, 3382 (1984); B. Persson and A. Liebsch, Phys. Rev. B **28**, 4247 (1983); D. Bedeaux and J. Vlieger, Physica **73**, 287 (1974); B. Felderhoff and R. Jones, Z. Phys. B **62**, 43 (1985).

[9]M. Quinten, U. Kreibig, D. Schönauer, and L. Genzel, Surf. Sci. **156**, 741 (1985); M. Quinten and U. Kreibig, Surf. Sci. **172**, 557 (1986); U. Kreibig, Z. Phys. D **3**, 239 (1986).

[10]Ag hydrosols as used for the present investigation have A_1 bands which are always broader than the calculated ones. The bandwidth in Fig. 2(b) is therefore adapted to experimental spectra of an appropriate diluted system with well-separated particles [U. Kreibig, Z. Phys. B **31**, 39 (1978)].

[11]D. B. Tanner, A. J. Sievers, and R. A. Buhrman, Phys. Rev. B **11**, 1330 (1975); D. Tanner, Phys. Rev. B **30**, 1042 (1984).

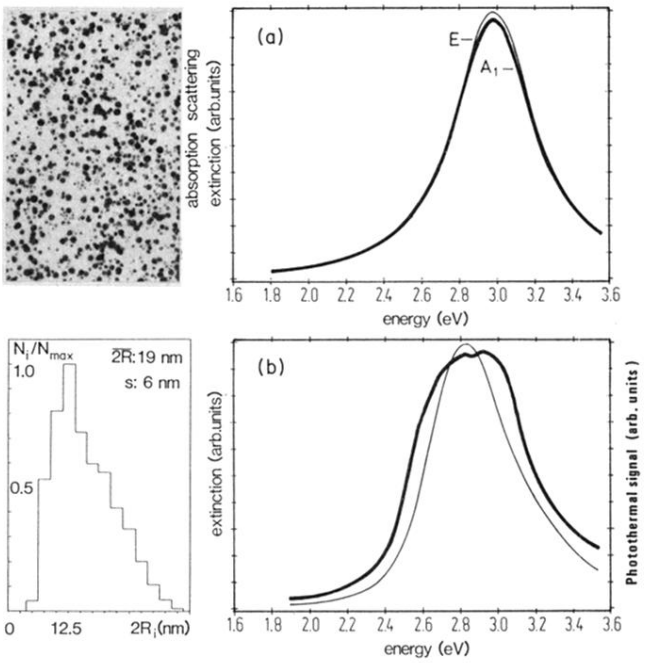

FIG. 2. Computed and measured optical spectra of a sample of small Ag particles ($\overline{2R} = 19 \pm 6$ nm). The left-side figures show a TEM picture and the size distribution of the measured sample. (a) Computed Mie extinction (E) and dipolar absorption (A_1). (Filling factor $= 10^{-6}$; size distribution included; dielectric constant of the matrix is 2.37; see Ref. 10). (b) Measured extinction spectrum (thin line) and photothermal spectrum (bold line).

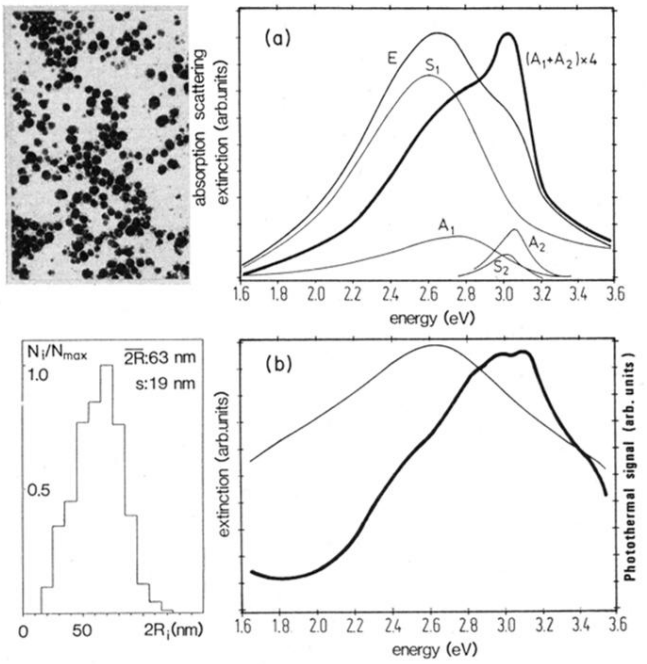

FIG. 3. Computed and measured optical spectra of a sample of larger Ag particles ($\overline{2R} = 63 \pm 19$ nm). The left-side figures show a TEM picture and the size distribution of the measured sample. (a) Computed Mie extinction (E) and the contributions of the ν-polar absorption (A_ν) and scattering (S_ν) bands. The total true absorption is plotted on an $4\times$ enlarged scale (bold line). (Filling factor is 10^{-6}; size distribution included; dielectric constant of the matrix is 2.37). (b) Measured extinction spectrum (thin line) and photothermal spectrum (bold line).